

Computational Studies on Pseudorotaxanes by Molecular Dynamics and Free Energy Perturbation Simulations

Xavi Grabuleda, Petko Ivanov,[†] and Carlos Jaime*

Department of Chemistry, Faculty of Sciences, Universitat Autònoma de Barcelona, 08193 Bellaterra, Spain

carlos.jaime@uab.es

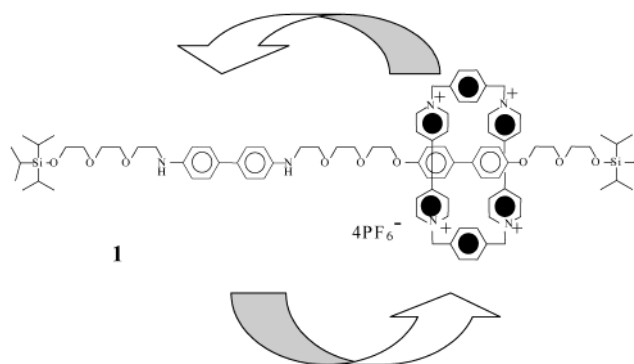
Received October 14, 2002

A computational scheme that comprises the utilization of the AMBER force field with RESP charges and an explicit solvent model for acetonitrile proved to be useful for studying the structures and energetics of pseudorotaxanes of benzidine and 4,4'-biphenol with cyclobis(paraquat-*p*-phenylene). The scheme can be further utilized for modeling [2]rotaxanes.

Introduction

Since the preparation of the first [2]rotaxane, **1**, operating as a switcher at the molecular level (a controllable molecular shuttle comprising a molecular ring threaded on an axle containing two "docking points") that can be activated chemically and electrochemically,¹ research in this area has evolved tremendously. Rotaxanes have been used for developing chemically, electrochemically, and photochemically driven molecular machines,² dendrimers,³ molecular machines able to produce optical responses from a chemical stimulus,⁴ logical ports capable of executing the XO⁵ and XNO⁶ functions, molecular cables,⁷ and a capability for switching a chiral optical response "on" or "off".⁸ The future of molecular machines

was thus announced.⁹ We are now dealing with the second generation of these machines: they have been synthesized on surfaces,^{2c,10,11} even forming a two-dimensional crossbar circuit configured for logic applications;¹² they have been self-assembled at air–water interfaces to avoid the problems that molecular machines present in solution^{2c,13} and they have been used to fabricate solid-state devices from Langmuir Blodgett molecular monolayers.¹⁴ The construction of logical gates from molecular switches formed by monolayers activated by redox processes and placed between metallic electrodes has also been described.¹⁵ Publication of these data paved the way to the CAENs (chemically assembled electronic nanocomputers), an alternative to the architecture of actual integrated circuits,¹⁵ a strategy that has intrinsic limitations.¹⁶ From this point, we move on to computers based on molecular-level components, and it seems that a very small step is needed.¹⁷



In contrast to this fascinating development of the experimental work based on rotaxanes, computational studies aimed at predicting and rationalizing the switch-

[†] On a sabbatical leave from the Institute of Organic Chemistry with Centre of Phytochemistry, Bulgarian Academy of Sciences, Sofia, Bulgaria.

(1) Bissell, R. A.; Córdova, E.; Kaifer, A. E.; Stoddart, J. F. *Nature* **1994**, *369*, 133–137.

(2) (a) Ballardini, R.; Balzani, V.; Gandolfi, M. T.; Prodi, L.; Venturi, M.; Philp, D.; Ricketts, H. G.; Stoddart, J. F. *Angew. Chem., Int. Ed. Engl.* **1993**, *32*, 1301–1303. (b) Benniston, A. C.; Harriman, A. *Angew. Chem., Int. Ed. Engl.* **1993**, *32*, 1459–1461. (c) Balzani, V.; Credi, A.; Raymo, F. M.; Stoddart, J. F. *Angew. Chem., Int. Ed.* **2000**, *39*, 3348–3391 and references therein. (d) Ballardini, R.; Balzani, V.; Credi, A.; Gandolfi, M. T.; Ventura, M. *Acc. Chem. Res.* **2001**, *34*, 445–455. (e) Schalley, C. A.; Beizai, K.; Vögtle, F. *Acc. Chem. Res.* **2001**, *34*, 465–476.

(3) Amabilino, D. B.; Ashton, P. R.; Bělohradský, M.; Raymo, F. M.; Stoddart, J. F. *J. Chem. Soc., Chem. Commun.* **1995**, 751–754.

(4) (a) Asakawa, M.; Iqbal, S.; Stoddart, J. F.; Tinker, N. D. *Angew. Chem., Int. Ed. Engl.* **1996**, *35*, 976–978. (b) Ballardini, R.; Balzani, V.; Credi, A.; Gandolfi, M. T.; Langford, S. J.; Menzer, S.; Prodi, L.; Stoddart, J. F.; Venturi, M.; Williams, D. J. *Angew. Chem., Int. Ed. Engl.* **1996**, *35*, 978–981.

(5) Credi, A.; Balzani, V.; Langford, S. J.; Stoddart, J. F. *J. Am. Chem. Soc.* **1997**, *119*, 2679–2681.

(6) Asakawa, M.; Ashton, P. R.; Balzani, V.; Credi, A.; Mattersteig, G.; Matthews, O. A.; Montalti, M.; Spencer, N.; Stoddart, J. F.; Venturi, M. *Chem. Eur. J.* **1997**, *3*, 1992–1996.

(7) (a) Ashton, P. R.; Ballardini, R.; Balzani, V.; Constable, E. C.; Credi, A.; Kocian, O.; Langford, S. J.; Preece, J. A.; Prodi, L.; Schofield, E. R.; Spencer, N.; Stoddart, J. F.; Wenger, S. *Chem. Eur. J.* **1998**, *4*, 2413–2422. (b) Ballardini, R.; Balzani, V.; Clemente-León, M.; Credi, A.; Gandolfi, M. T.; Ishow, E.; Perkins, J.; Stoddart, J. F.; Tseng, H.-R.; Wenger, S. *J. Am. Chem. Soc.* **2002**, *124*, 12786–12795.

(8) Asakawa, M.; Brancato, G.; Fantì, M.; Leigh, D. A.; Shimizu, T.; Slavin, A. M. Z.; Wong, J. K. Y.; Zerbetto, F.; Zhang, S. *J. Am. Chem. Soc.* **2002**, *124*, 2939–2950.

(9) (a) Balzani, V.; Gómez-López, M.; Stoddart, J. F. *Acc. Chem. Res.* **1998**, *31*, 405–414. (b) Shipway, A. N.; Willner, I. *Acc. Chem. Res.* **2001**, *34*, 421–432.

(10) Laitenberger, P.; Claessens, C. G.; Kuipers, F. M.; Raymo, F. M.; Palmer, R. E.; Stoddart, J. F. *Chem. Phys. Lett.* **1997**, *279*, 209–214.

ing processes are rare. The literature offers articles where computational studies on rotaxanes are embedded into largely more detailed experimental results.¹⁸ Most of them are devoted to systems where cyclodextrins are the macrocycle,¹⁹ although catenanes have also been considered.²⁰ However, several articles present computational studies on the complexation process between cyclobis(paraquat-*p*-phenylene) and aromatic guests²¹ and also phenyl glucosides.²² In particular, such studies have shown the advantage of simulation methods (Monte Carlo)^{21b} over simple energy minimizations. The development of computational approaches for studying these interesting systems will undoubtedly open up new directions of interest and research.

The results obtained so far make clear the necessity for improvements in the simulation protocols along two lines: (a) the modeling of the electrostatic interactions and (b) the effect of the solvent (usually acetonitrile). Empirical force field calculations have to be able to adequately consider these two main aspects in order to further improve their application in studies of much more complex and larger systems such as the ones being prepared nowadays based on [*n*]rotaxanes and [*n*]catenanes.^{11,12} The importance of the C–H···O hydrogen bonding in molecular and supramolecular structures has also been stressed.²³ We have shown recently that the AMBER* force field reproduces short C–H···O contacts in [2]rotaxanes.²⁴ Additionally, we reported a new six-site solvent model for acetonitrile²⁵ (the major solvent used in rotaxane chemistry) based on the AMBER scheme.

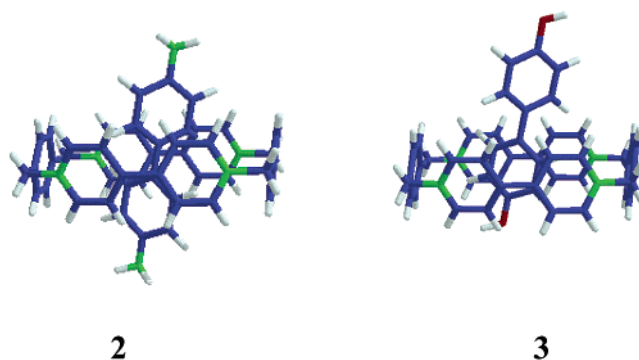


FIGURE 1. Inclusion complexes between cyclobis(paraquat-*p*-phenylene) and benzidine, **2**, and 4,4'-biphenol, **3**.

With this work, we intend to establish a computational methodology aimed at studying the shuttling process observed in [2]rotaxanes. More specifically, the supramolecular geometry of the pseudorotaxanes formed by inclusion of benzidine and 4,4'-biphenol into cyclobis(paraquat-*p*-phenylene), **2** and **3**, respectively, will be studied. The free energy difference pertaining to these complexation processes will also be estimated. The aromatic “station” of benzidine (pseudorotaxane **2**) displays a clearly pronounced stronger preference for complexation as compared with 4,4'-biphenol (**3**). The association constants estimated experimentally are, 1044 and 140 M⁻¹ for **2** and **3**, respectively.²⁶ These aromatic residues can be incorporated into a polyether chain, thus yielding [2]rotaxane **1**, and accordingly, they can be considered as pieces of a potential molecular machine (nanoscale molecular switches and information-storing devices).^{21b} Results of computer simulations also provide valuable information regarding the prevailing intermolecular interactions responsible for the molecular recognition in supramolecular systems.^{21b}

We can evaluate indirectly the free energy difference between two reactions by computing the free energies involved in two fictitious reactions representing the mutation of one substrate into the other by a series of small reversible changes. These mutations are simulated by the free energy perturbation (FEP) method.²⁷ This methodology is preferentially used when the two reactions are too difficult to be studied by standard computational methods. Typical applications of FEP comprise the estimation of solvation energies^{28,29} and reactivity,³⁰ although it has also been applied to the study of ligand–receptor interactions.³¹

We present here the results from studies with molecular dynamics (MD) simulations and FEP methods on the two pseudorotaxanes, **2** and **3** (Figure 1), formed by the inclusion of electron-rich aromatic subunits (benzi-

(11) Chia, S.; Cao, J.; Stoddart, J. F.; Zink, J. I. *Angew. Chem., Int. Ed.* **2001**, *40*, 2447–2451.

(12) Luo, Y.; Collier, C. P.; Jeppesen, J. O.; Nielsen, K. A.; Delonno, E.; Ho, G.; Perkins, J.; Tseng, H.-R.; Yamamoto, T.; Stoddart, J. F.; Heath, J. R. *ChemPhysChem* **2002**, *3*, 519–525.

(13) (a) Ahuja, R. C.; Caruso, P.-L.; Möbius, D.; Wildburg, G.; Ringsdorf, H.; Philp, D.; Preece, J. A.; Stoddart, J. F. *Langmuir* **1993**, *9*, 1534–1544. (b) Pease, A. R.; Jeppesen, J. O.; Stoddart, J. F.; Luo, Y.; Collier, C. P.; Heath, J. R. *Acc. Chem. Res.* **2001**, *34*, 433–444.

(14) Collier, C. P.; Jeppesen, J. O.; Luo, Y.; Perkins, J.; Wong, E. W.; Heath, J. R.; Stoddart, J. F. *J. Am. Chem. Soc.* **2001**, *123*, 12632–12641.

(15) Collier, C. P.; Wong, E. W.; Bělohradský, M.; Raymo, F. M.; Stoddart, J. F.; Kuekes, P. J.; Williams, R. S.; Heath, J. R. *Science* **1999**, *285*, 391–394.

(16) See the special issue on nanoscale materials, guest editor J. R. Heath in *Acc. Chem. Res.* **1999**, *32*, all pages.

(17) (a) Ball, P. *Nature* **2000**, *406*, 118–120. (b) Pease, A. R.; Stoddart, J. F. *Struct. Bonding (Berlin)* **2001**, *99*, 189–236.

(18) As examples, see: (a) Amabilino, D. B.; Asakawa, M.; Ashton, P. R.; Ballardini, R.; Balzani, V.; Belohradský, M.; Credi, A.; Higuchi, M.; Raymo, F. M.; Shimizu, T.; Stoddart, J. F.; Venturi, M.; Yase, K. *New J. Chem.* **1998**, *22*, 959–972. (b) Ashton, P. R.; Boyd, S. E.; Menzer, S.; Pasini, D.; Raymo, F. M.; Spencer, N.; Stoddart, J. F.; White, A. J. P.; Williams, D. J.; Wyatt, P. G. *Chem. Eur. J.* **1998**, *4*, 299–310.

(19) (a) Mayer, B.; Klein, C. T.; Topchieva, I. N.; Kohler, G. *J. Comput. Aid. Mol. Design* **1999**, *13*, 373–383. (b) Pozuelo, J.; Mendi-cuti, F.; Saiz, E. *Polymer* **2001**, *43*, 523–531. (c) Pozuelo, J.; Mendi-cuti, F.; Mattice, W. L. *Polym. J.* **1998**, *30*, 479–484. (d) Pozuelo, J.; Mendi-cuti, F.; Mattice, W. L. *Macromolecules* **1997**, *30*, 3685–3690. (e) Horsky, J. *Macromol. Theory Simul.* **2000**, *9*, 759–771.

(20) Raymo, F. M.; Houk, K. N.; Stoddart, J. F. *J. Org. Chem.* **1998**, *63*, 6523–6528.

(21) (a) Zhang, K.-C.; Liu, L.; Mu, T.-W.; Guo, Q.-X. *Chem. Phys. Lett.* **2001**, *333*, 195–198. (b) Kaminski, G. A.; Jorgensen, W. L. *J. Chem. Soc., Perkin Trans. 2* **1999**, 2365–2375. (c) Castro, R.; Davidov, P. D.; Kumar, K. A.; Marchand, A. P.; Evanseck, J. D.; Kaifer, A. E. *J. Phys. Org. Chem.* **1997**, *10*, 369–382.

(22) Lipton, M. A. *Tetrahedron Lett.* **1996**, *37*, 287–290.

(23) Raymo, F. M.; Bartberger, M. D.; Houk, K. N.; Stoddart, J. F. *J. Am. Chem. Soc.* **2001**, *123*, 9264–9267.

(24) Grabuleda, X.; Jaime, C. *J. Org. Chem.* **1998**, *63*, 9635–9643.

(25) Grabuleda, X.; Jaime, C.; Kollman, P. A. *J. Comput. Chem.* **2000**, *21*, 901–908.

(26) Córdova, E.; Bissell, R. A.; Spencer, N.; Ashton, P. R.; Stoddart, J. F.; Kaifer, A. E. *J. Org. Chem.* **1993**, *58*, 6550–6552.

(27) Kollman, P. A. *Chem. Rev.* **1993**, *93*, 2395–2417.

(28) Miller, J. L.; Kollman, P. A. *J. Phys. Chem.* **1996**, *100*, 8587–8594.

(29) Meng, E. C.; Caldwell, J. W.; Kollman, P. A. *J. Phys. Chem.* **1996**, *100*, 2367–2371.

(30) Pearlman, D. A.; Connely, P. R. *J. Mol. Biol.* **1995**, *148*, 696–717.

(31) Mezei, M.; Beveridge, D. L. *Ann. N. Y. Acad. Sci.* **1986**, *482*, 1–23.

dine and 4,4'-biphenol, respectively) in an electron-deficient receptor, cyclobis(paraquat-*p*-phenylene). The good behavior of the methodology followed in this work warrants success in the computational study of the shuttling process of the already well-known [2]rotaxanes.

Computational Methodology

MD simulations were carried out using the SANDER module of the AMBER v.5 program.³² The parm94 force field was used throughout this work.³³ Simulations were performed in the gas phase and in water and acetonitrile as explicit solvents. The presence or the absence of counterions (chlorides) was also considered in the simulations. Productive runs of 400 ps length were used for the isolated host and guests. A cutoff of 10.0 Å was used for the long-range nonbonding interactions in the gas phase and in the water simulations, while two cutoffs at 13.0 and 16.0 Å were assumed for the simulations in acetonitrile.

Explicit TIP3P water molecules were included in the simulations carried out in water.³⁴ Our acetonitrile solvent model was used for the MD simulations in acetonitrile.²⁵ Periodic boundary conditions were always applied to the system when the solvent was taken into consideration. The distribution of solvent molecules around the complexes was analyzed with the CARNAL module of the AMBER program.

The acetonitrile solvent model was developed with two different sets of RESP atomic charges depending on the basis set used: HF/6-31G* or HF/6-311+G*. All computations were performed with both sets of charges.³⁵ However, only the HF/6-311+G* results will be described because they more effectively reproduce the known geometry and energy data of pseudorotaxanes **2** and **3**.

The GIBBS module of AMBER and the windows method were used for the FEP computations. Although the *slow-growth* method is conceptually better, there are indications that the latter method is not sufficiently accurate due to inconsistencies in the Hamiltonian.³⁶ The thermodynamic cycle studied is shown in Figure 2. The width of the windows was always 0.02 (51 windows). Equilibration and productive cycles (2500 each) were executed. In acetonitrile, the number of equilibration and productive cycles per window was 3500.

Force Field Parametrization. The electrostatic interactions in the AMBER force field are estimated using RESP charges. The RESP charges are obtained by fitting the ab initio molecular electrostatic potential (charges derived from a HF/6-31G* wavefunction in our case)^{37,38} after introducing some

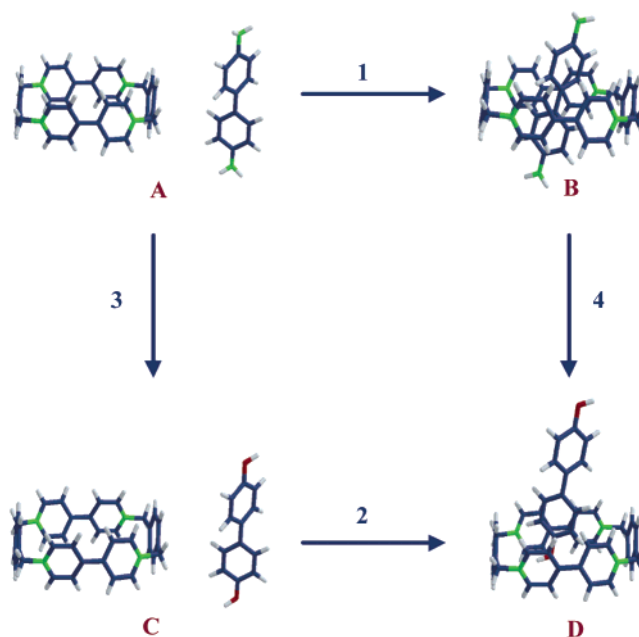


FIGURE 2. Thermodynamic cycle involving the studied pseudorotaxanes ($\Delta G_1 - \Delta G_2 = \Delta G_3 - \Delta G_4$).

restrictions based on equivalences of conformations due to symmetry. The RESP charges are thus independent of the molecular conformation. The atomic charges used in the computations are presented in Figure 3.³⁹ The size of the macrocycle was too large to be geometry optimized with HF/6-31G*. Single-point calculations were carried out on this system using crystallographic coordinates⁴⁰ because when aromatic fragments are present a higher level of theory in the ab initio computations is necessary in order to correctly reproduce the geometrical data of the system.⁴¹ An alternative approach was also attempted: for obtaining the RESP charges, the macrocycle was considered as being composed of two basic fragments, *p*-xylyl and paraquat (PQT²⁺). Unsatisfactory results were obtained: these charges significantly deviate from values already implemented in the force field for similar molecular fragments, and we considered them to be inappropriate for our study.

Some additional force field parameters for bond stretching, angle bending, torsions, and improper torsions were developed on the basis of the X-ray structure of the macrocycle. Moreover, the FEP method requires the utilization of dummy atoms. The parameters used for these computations are given in Supporting Information as a table. More details will be further given in the text for each particular case.

Results and Discussion

Simulations for Isolated Species in the Gas Phase.

The simulation protocol for the macrocyclic receptor consisted of three steps: (i) an initial minimization (1000 cycles) for adjusting the positions of the counterions, (ii) full geometry optimization of the system with the purpose of releasing the strain present in the structure; and (iii)

(39) Comparison of our computed charges with those contained in the parm94 force field of AMBER shows similar values for the different functional groups studied, e.g., the charges for adenine present values -0.912 for N and 0.417 for its hydrogens. Analogously, the charge for the hydroxylic oxygen of tyrosine is -0.558 and that for its hydrogen is 0.399 .

(40) (a) Allwood, B. L.; Spencer, N.; Shahriari-Zavareh, H.; Stoddart, J. F.; Williams, D. J. *J. Chem. Soc., Chem. Commun.* **1987**, 1061–1064. (b) Stoddart, J. F. *Pure Appl. Chem.* **1988**, *60*, 467–472.

(41) Ivanov, P. M. *J. Mol. Struct.* **1997**, *415*, 179.

(32) Case, D. A.; Pearlman, D. A.; Caldwell, J. W.; Cheatham, T. E., III; Ross, W. S.; Simmerling, C. L.; Darden, T. A.; Merz, K. M.; Stanton, R. V.; Cheng, A. L.; Vincent, J. J.; Crowley, M.; Ferguson, D. M.; Radmer, R. J.; Seibel, G. L.; Singh, U. C.; Weiner, P. K.; Kollman, P. A. AMBER 5; University of California–San Francisco, San Francisco, 1997.

(33) Cornell, W. D.; Cieplak, P.; Bayly, C. I.; Gould, I. R.; Merz, K. M.; Ferguson, D. M.; Spellmeyer, D. C.; Fox, T.; Caldwell, J. W.; Kollman, P. A. *J. Am. Chem. Soc.* **1995**, *117*, 5179–5197.

(34) Jorgensen, W. L.; Chandrasekhar, J.; Madura, J. D.; Impey, R. W.; Klein, M. L. *J. Chem. Phys.* **1983**, *79*, 926–935.

(35) Grabuleda, X., Ph.D. Thesis, Universitat Autònoma de Barcelona, Barcelona, 2000.

(36) Pearlman, D. A.; Kollman, P. A. *J. Chem. Phys.* **1989**, *91*, 7831–7839.

(37) Frisch, M. J.; Trucks, G. W.; Schlegel, H. B.; Gill, P. M. W.; Johnson, B. G.; Robb, M. A.; Cheeseman, J. R.; Keith, T.; Petersson, G. A.; Montgomery, J. A.; Raghavachari, K.; Al-Laham, M. A.; Zakrzewski, V. G.; Ortiz, J. V.; Foresman, J. B.; Cioslowski, J.; Stefanov, B. B.; Nanayakkara, A.; Challacombe, M.; Peng, C. Y.; Ayala, P. Y.; Chen, W.; Wong, M. W.; Andres, J. L.; Replogle, E. S.; Comperts, R.; Martin, R. L.; Fox, D. J.; Binkley, J. S.; Defrees, D. J.; Baker, J.; Stewart, J. P.; Head-Gordon, M.; Gonzalez, C.; Pople, J. A. *Gaussian 94* (revision A.1); Gaussian, Inc.: Pittsburgh, PA, 1995.

(38) Geometry was optimized with the HF/6-31G* basis set, and the molecular electrostatic potential was computed using the keywords iop(6/33) = 2 and Pop = mk (Besler, B. H.; Merz, K. M.; Kollman, P. A. *J. Comput. Chem.* **1990**, *11*, 431–439).

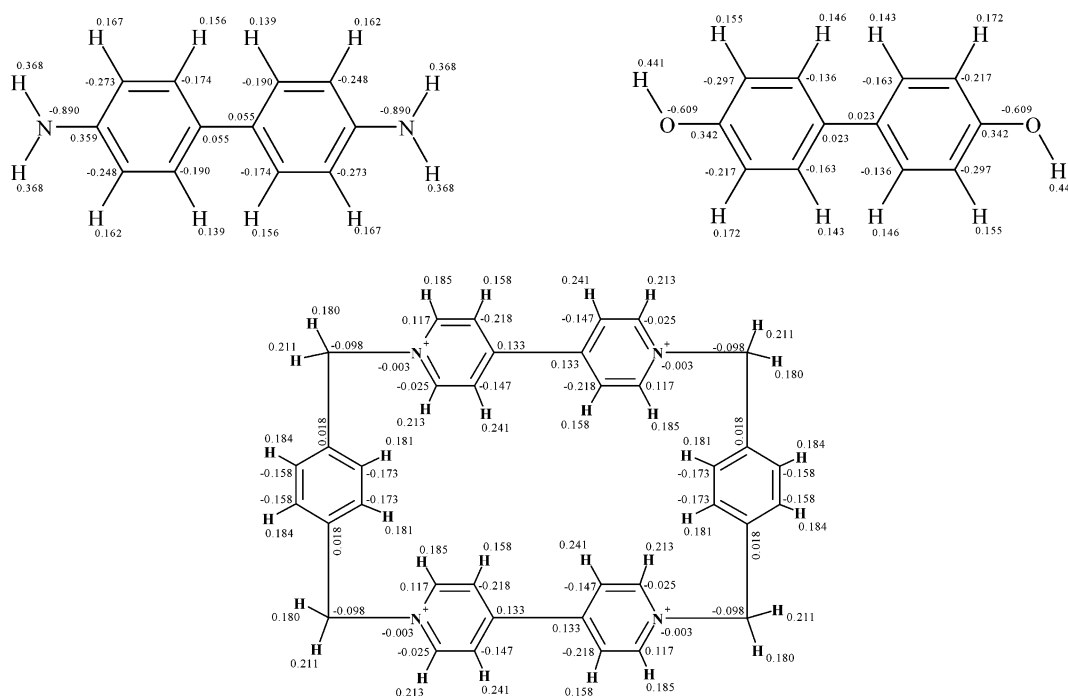


FIGURE 3. RESP charges for the benzidine, 4,4'-biphenol, and cyclobis(paraquat-*p*-phenylene).

TABLE 1. Average Energies (kcal/mol) Obtained from MD Simulations in the Gas Phase of the Tetracationic Macrocycle with and without Counterions

counterions	E_{pot}	E_{stret}	E_{bend}	E_{tors}	E_{vdW}	E_{elec}	$E_{1-4 \text{ vdW}}$	$E_{1-4 \text{ elec}}$
with Cl^-	-29.9	15.5	22.8	25.5	5.2	-168.9	27.8	42.2
without Cl^-	494.4	19.2	25.6	25.9	-5.6	360.3	27.5	41.7

TABLE 2. Structural Parameters for Cyclobis(paraquat-*p*-phenylene)^a (Distances in Å and Angles in Degrees)

	a	b	c	d	e	f
X-ray	108	14	23	19	10.3	6.8
with Cl^-	108	7	13	2	10.3	7.0
without Cl^-	108	7	12	1	10.3	7.0

^a See Figure 4a for the meaning of the geometric parameters.

MD simulation after heating the system to 298 K, followed by an equilibration run for 100 ps, and a production run (400 ps). SHAKE was applied to all bonds containing hydrogens. The velocities obtained at the end of these simulations were used for the FEP computations.

The system is largely stabilized by the presence of the counterions, as reflected in the long-range electrostatic contribution (E_{elec}) (Table 1). Both MD simulations maintained the shape of the macrocycle (a slightly curved rectangular box), with geometrical values closely matching the available experimental X-ray data⁴⁰ (Table 2).

The twisting and the bending of the bipyridyl moieties are, however, underestimated, and these discrepancies could be partly due to the crystal packing.²¹ Starting with a homogeneous distribution of the Cl^- ions outside and in front of the paraquat units, the MD simulation renders one chloride anion opposing each paraquat unit, and the other two anions are rendered at the two cavity entrances (Figure 4).

Simulations for Pseudorotaxanes 2 and 3 in the Gas Phase. The component molecules separated from

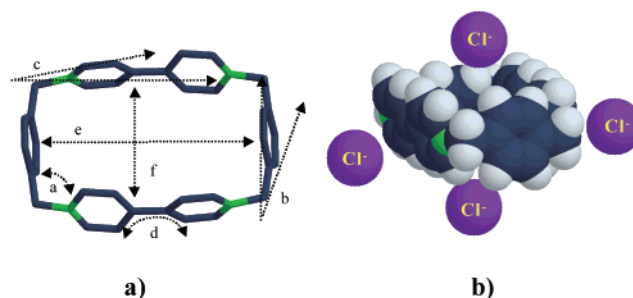
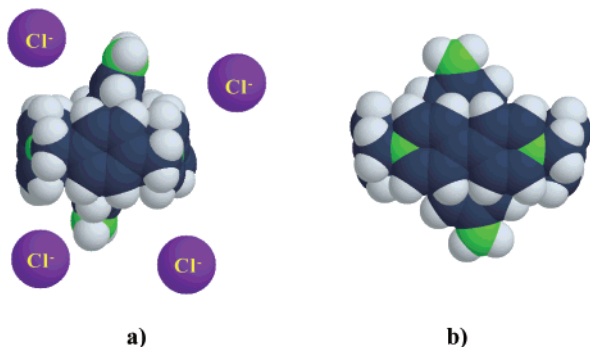
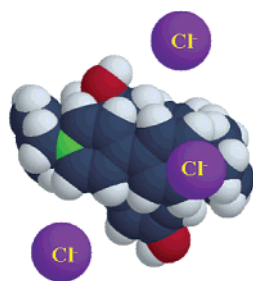


FIGURE 4. Cyclobis(paraquat-*p*-phenylene). (a) Schematic representation with a designation of the geometrical parameters given in Table 2. (b) Snapshot showing the distribution of the chloride ions after the MD simulation; chlorides on the right and on the left are in front of the paraquat units, while the upper and lower ones are at the cavity entrances.

each other during the simulations of **2** and **3** in the gas phase and in water. Since NOE experiments²⁶ indicate the formation of a complex, we imposed restrictions on the guest and the host movements. The formation of **2** and **3** is favored mainly by the long-range van der Waals interactions (Table 3; compare with the data in Table 1). The long-range electrostatics slightly disfavor the complexes when counterions are present, and this significantly lowers the energy of the systems in the absence of counterions. The experimentally proposed geometry²⁶ of **2** is reproduced in the two simulations. The benzidine aromatic rings are positioned symmetrically with respect to the center of the cavity. The geometrical center of the

TABLE 3. Average Energies (kcal/mol) Obtained from MD Simulations in the Gas Phase of Pseudorotaxanes **2** and **3** in the Presence and in the Absence of Counterions

product	counterions	E_{pot}	E_{stret}	E_{bend}	E_{tors}	E_{vdW}	E_{elec}	$E_{1-4 \text{ vdW}}$	$E_{1-4 \text{ elec}}$
2	with Cl^-	-56.5	21.3	32.3	33.3	-14.3	-163.2	37.2	-3.6
	without Cl^-	400.5	17.1	24.1	22.0	-25.9	331.5	35.4	-3.9
3	with Cl^-	-33.5	22.0	31.5	33.8	-12.0	-160.3	36.2	14.6
	without Cl^-	421.0	16.2	25.1	20.1	-25.1	341.0	34.4	12.9

**FIGURE 5.** CPK representation of the average structure of pseudorotaxane **2** obtained in the MD simulations in the gas phase: (a) side view for the simulation with counterions; (b) front view for the simulation without counterions.**FIGURE 6.** CPK representation of the average structure of pseudorotaxane **3** obtained in the MD simulations in the gas phase and in the presence of chloride ions.

guest is only 0.7 Å from it. These results oppose the X-ray geometry of **2**.^{21b} The chloride anions escape from the paraquat moieties and prefer to be nearer to the benzidine rings in **2** (Figure 5), while two pairs of anions are located near each of the hydroxyl hydrogens in **3** (average distance = 5.3 Å) and at both sides of the paraquat units (Figure 6; average distance 6.8 Å), respectively.

The stretch, bend, and torsion deformations increase the energy when the chloride ions are included. It seems that the presence of these ions in close proximity to the complexes produces steric compression and deformations. The interactions between the guest and the chloride ions are primarily responsible for these deformations of the intramolecular coordinates. Irrespective of the increase of the structural strain, the presence of the chloride ions greatly stabilizes both pseudorotaxanes.

The substrate of **3** has greater mobility than the one in **2**. The distance between the center of the macrocycle cavity and the geometrical center of the guest is 1.1 Å in **3** (Figure 6). This is an indication for different geometries of the inclusion complexes **2** and **3**, again in agreement with the experimentally proposed geometries.²⁶

Simulations for Pseudorotaxanes 2 and 3 in Water as a Solvent. The presence of water molecules

did not significantly affect the geometries of the complexes and the molecules: pseudorotaxane **2** has the two aromatic rings of the benzidine moiety equidistantly positioned with respect to the equatorial plane of the macrocycle. The average distances between the macrocycle center of gravity and the guest aromatic rings centers are 2.4 and 1.9 Å in the presence of chloride ions and 2.3 and 2.0 Å in the absence of chloride ions (Figure 7 depicts the variations of these distances). All four chlorides are about 11.1 ± 4.3 Å from the center of the cavity. The integration of the radial distribution functions for the distances $\text{N} \cdots \text{H}_2\text{O}$ and $\text{NH} \cdots \text{OH}_2$ (Figure 8) gave about 44 water molecules in the proximity of the pseudorotaxane at a distance less than 4.5 Å. The sharpness of the first pick for the $\text{NH} \cdots \text{OH}_2$ plot indicates a certain rigidity of the system.

Pseudorotaxane **3** has an average geometry quite different from that of **2** (Figure 9). The average distances when counterions are present are 2.8 and 1.6 Å for the farthest and nearest rings, respectively. A tendency for one of the aromatic rings to remain preferentially in the cavity of the cyclophane is clearly portrayed at the final stage of the simulation. When counterions are not present, the average distances are 2.3 and 2.0 Å, thus showing no differences compared with complex **2**. The chloride anions are positioned closer to the center of the macrocycle and characterized by smaller variations, 10.1 ± 1.1 Å. The $\text{O} \cdots \text{H}_2\text{O}$ distribution is very similar to that of **2**, while the $\text{OH} \cdots \text{OH}_2$ distribution presents a sharper maximum for the first solvation shell (Figure 10), indicating strong electrostatic attractions between these two groups. The differences in shape for the radial distributions of $\text{O} \cdots \text{H}_2\text{O}$ and $\text{OH} \cdots \text{OH}_2$ contacts are due to a different number of interactions in each case: only one interaction between the hydroxylic oxygens and the water hydrogens and two interactions between the hydroxylic hydrogens and the water oxygens (the guest in **3** enters the cavity with one of the hydroxyl groups in the interior and protected by the crown of the cyclophane protons to be approached by water molecules).

Simulations for Pseudorotaxanes 2 and 3 in Acetonitrile. The inclusion of both guests in the macrocycle was studied in acetonitrile as the solvent, i.e., at conditions that closely resemble the experimental ones²⁶ except for the counterions.

We have to stress that the geometrical data of the macrocycle was more effectively reproduced when acetonitrile was used as the solvent. Most of the parameters in Table 2 remained almost unchanged. Only the torsion angles corresponding to the twisting of the two bipiridyl units (parameter d) changed from $1-2^\circ$ to the value of 10° (closer to the experimental estimate of 19°). This geometry parameter is the most sensitive one with respect to accounting for polarization and the presence or absence of counterions (see Table 5 of ref 21b). The

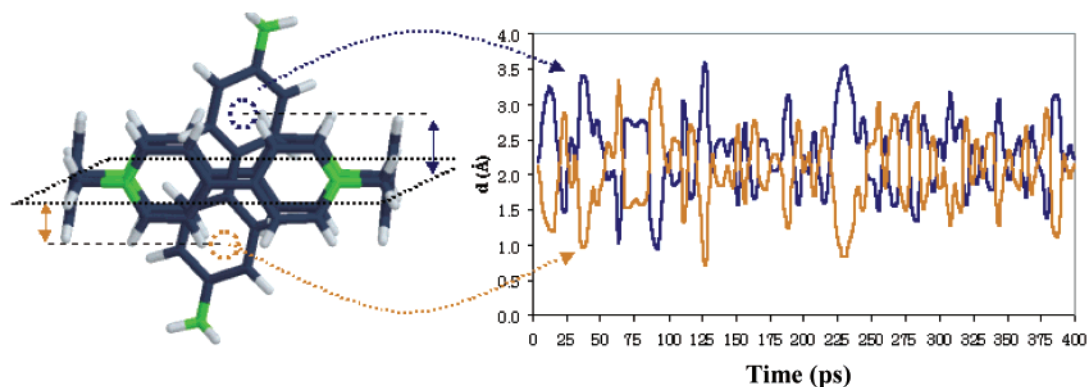


FIGURE 7. Variation of the indicated distances of pseudorotaxane **2** during the simulation (MD simulations carried out in the presence of counterions).

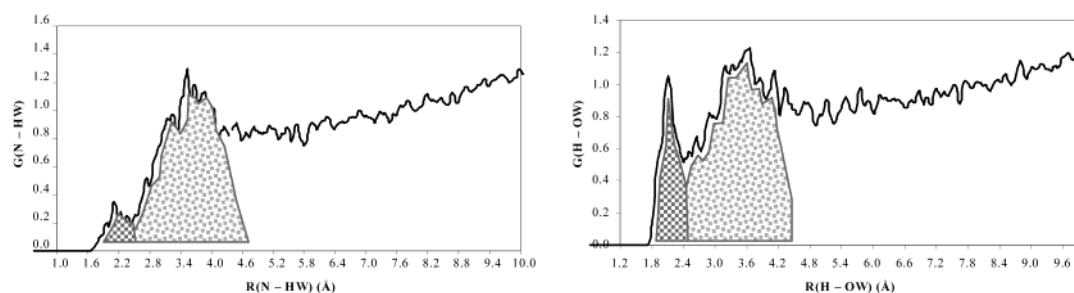


FIGURE 8. Radial distribution functions for selected distances between atoms of **2** and the water molecules. (a) $N\cdots H_2O$; (b) $NH\cdots OH_2$.

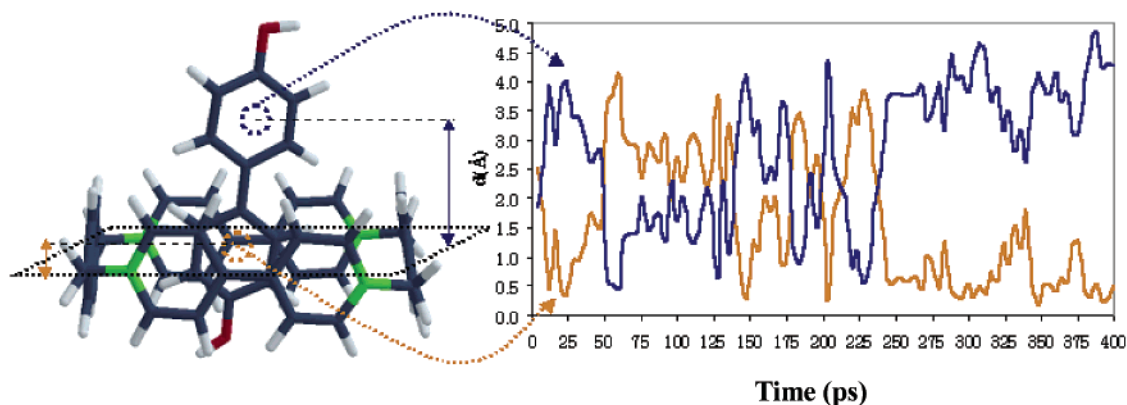


FIGURE 9. Variation of the indicated distances of pseudorotaxane **3** during the simulation (MD simulations carried out in the presence of counterions).

geometrical data for both guests were also well reproduced. No distance restrictions were necessary for the MD simulations of **2**, while **3** required such constraints to be imposed. Contrary to what was observed for **2** in the gas phase or in the in-water simulations, the complex remained stable in acetonitrile throughout the simulation time (a first indication for a greater stability).

The radial distribution function for the arrangement of acetonitrile molecules around pseudorotaxane **2** is shown in Figure 11. The solvent molecules nearest to the substrate orient their N atoms toward it. Figure 11a presents the distribution of the $N^+\cdots NC-CH_3$ interactions. The integral of the area up to 5.5 Å yielded the presence of about 32 solvent molecules in close proximity to the four cyclophanic nitrogens. Figures 11b and 11c

display the distribution of the solvent molecules around the amino functional groups of the benzidine unit. There is one maximum at 2.1 Å and another at 3.8 Å, with the total of three solvent molecules around each amino group. The distribution of solvent around the amino group, considered as a whole unit (Figure 11d), also corroborates these results.

The radial distribution function analysis of the solvent structure around pseudorotaxane **3** is presented in Figure 12. The curve in Figure 12a indicates that the solvent molecules in this case are distributed very similarly to the configuration they have in pseudorotaxane **2**. Solvent molecules (32) are positioned around the 4 nitrogens of the cyclophane. On the other hand, the number of close contacts between solvent molecules and the substrate is

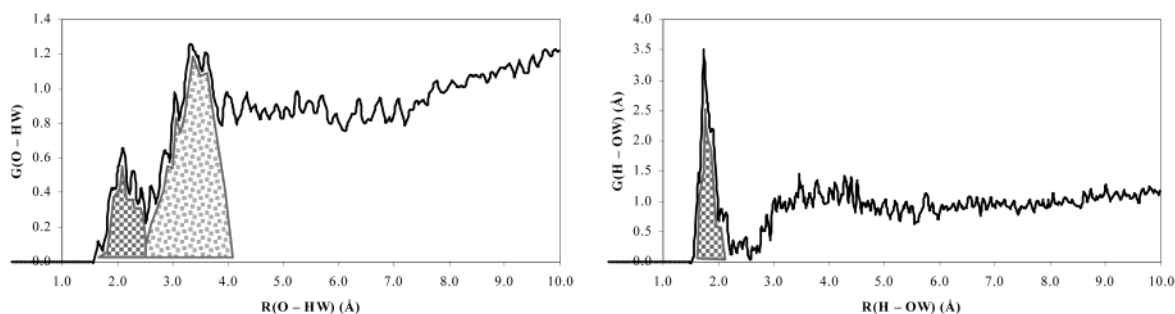


FIGURE 10. Radial distribution functions for selected distances between atoms of **3** and the water molecules. (a) $\text{O}\cdots\text{H}_2\text{O}$; (b) $\text{OH}\cdots\text{OH}_2$.

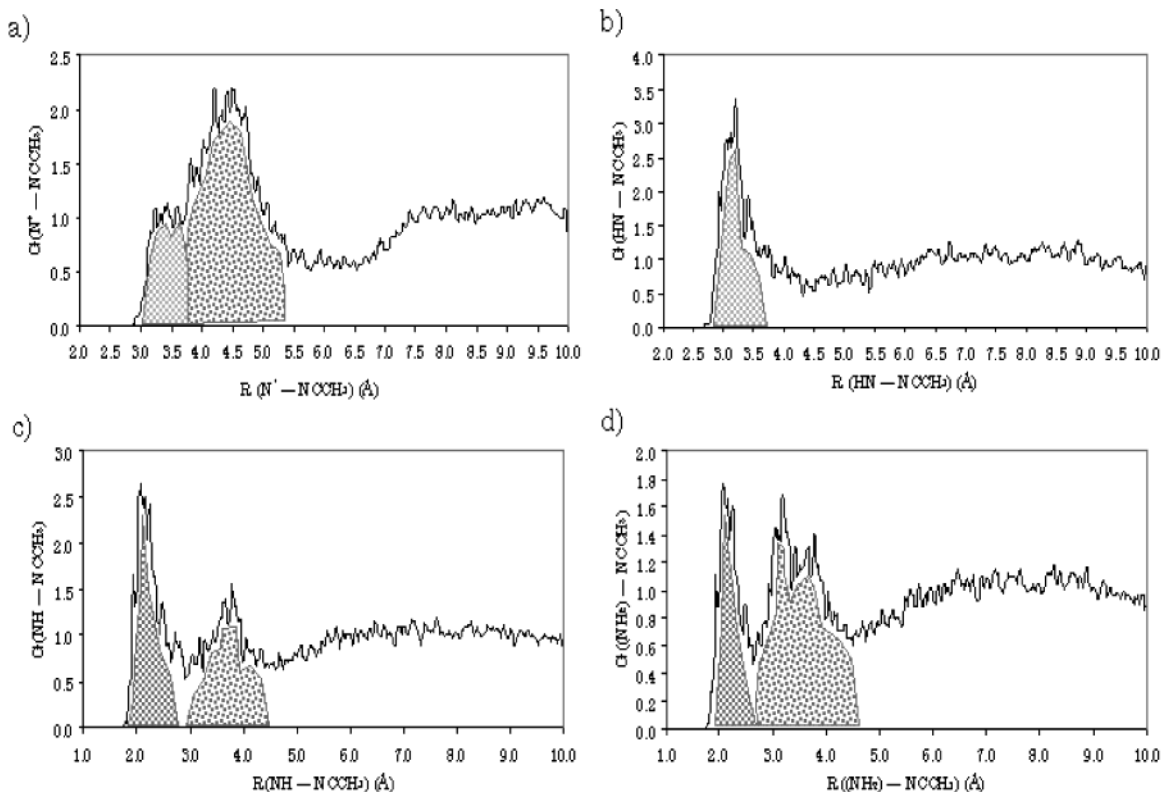


FIGURE 11. Radial distribution functions corresponding to the disposition of the solvent molecules around the pseudorotaxane **2**. (a) $\text{CH}_3\text{CN}\cdots\text{N}^+$; (b) $\text{CH}_3\text{CN}\cdots\text{N}(\text{benzidine})$; (c) $\text{CH}_3\text{CN}\cdots\text{H}_2\text{N}(\text{benzidine})$; (d) $\text{CH}_3\text{CN}\cdots\text{NH}_2(\text{benzidine})$; the amino group as a whole).

smaller in this case: only one acetonitrile molecule interacts with each hydroxylic hydrogen of the guest (Figures 12b and 12c). Moreover, the average distance between this solvent molecule and the guest is about 1.9 Å, i.e., it is 0.2 Å shorter than the corresponding distance in the case of **2**. The radial distribution functions for the distances between the acetonitrile methyl hydrogens and the oxygen atom of the biphenol moiety (Figure 12d) indicates the presence of 2–3 short contacts for each pair $\text{OH}\cdots\text{CH}_3\text{CN}$. It is worth noting here that such short contacts were not so markedly found in the distribution of solvent molecules around the pseudorotaxane **2**.

Free Energy Perturbation (FEP) Analysis. Table 4 contains the results obtained from all FEP simulations carried out in this work. The computed data are compared with the estimate of $\Delta G_1 - \Delta G_2$ (-1.2 kcal/mol)

for pseudorotaxanes **2** and **3** deduced from the experimentally determined association constants 1044 and 140 M^{-1} , respectively.²⁶

We have to stress that the results from these FEP calculations indicate the necessity of using counterions to order to obtain meaningful results. The higher stability of pseudorotaxane **2** in the gas phase compared with that of **3** was enhanced by about 7.0 kcal/mol when chloride ions were not present.

The results were also in disagreement with the experiment when the FEPs were carried out in the presence of water as the solvent: $\Delta G_1 - \Delta G_2$ is +0.8 kcal/mol in the presence of chloride ions and -0.17 kcal/mol when they were not included. An overestimation of the binding energy of complex **2** in the absence of counterions was obtained also in this case. The best results present the

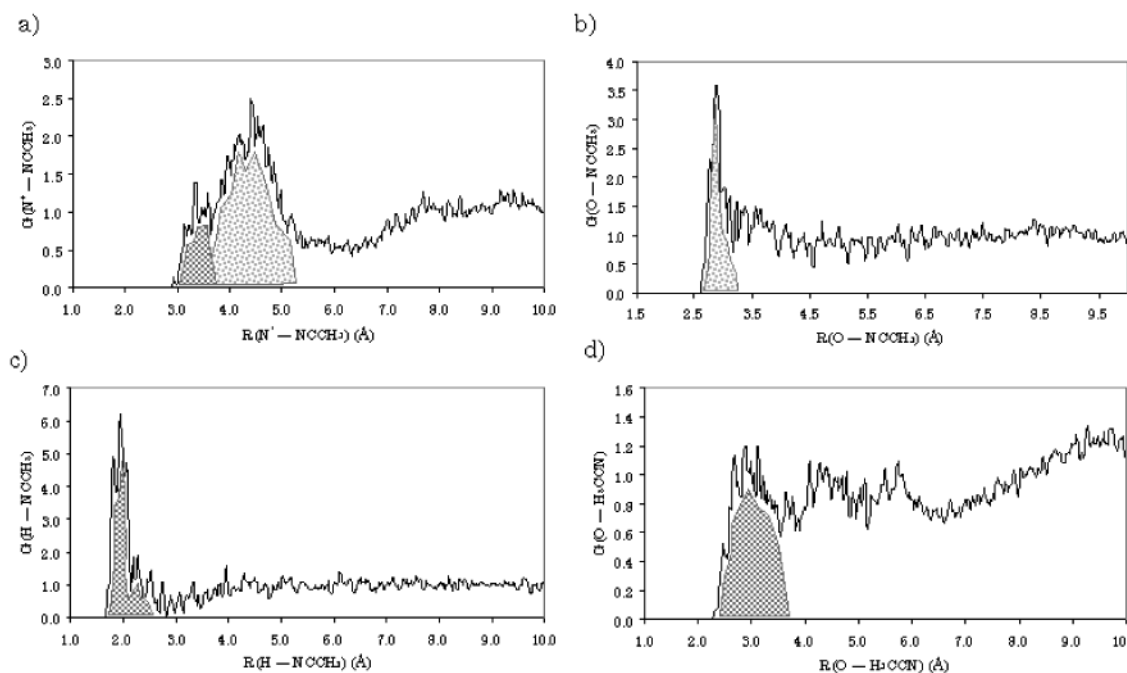


FIGURE 12. Radial distribution functions corresponding to the disposition of the solvent molecules around the pseudorotaxane **3**. (a) $\text{CH}_3\text{CN}\cdots\text{N}^+$; (b) $\text{CH}_3\text{CN}\cdots\text{O}(\text{biphenol})$; (c) $\text{CH}_3\text{CN}\cdots\text{HO}(\text{biphenol})$; (d) $\text{NC}-\text{CH}_3\cdots\text{OH}(\text{biphenol})$.

TABLE 4. Energy Values Obtained from FEP Simulations (kcal/mol) in Different Conditions

conditions	ΔG_3	ΔG_4	$\Delta G_3 - \Delta G_4 = \Delta G_1 - \Delta G_2$
experimental			-1.2
gas phase	20.41 ± 0.04	28.48 ± 0.03	-8.07 ± 0.03
gas phase + Cl^-	20.41 ± 0.04	20.95 ± 0.03	-0.54 ± 0.03
H_2O	15.46 ± 0.08	15.63 ± 0.01	-0.17 ± 0.05
$\text{H}_2\text{O} + \text{Cl}^-$	15.46 ± 0.08	14.66 ± 0.07	$+0.80 \pm 0.08$
CH_3CN	16.68 ± 0.03	18.23 ± 0.05	-1.55 ± 0.04
$\text{CH}_3\text{CN} + \text{Cl}^-$	16.68 ± 0.03	18.01 ± 0.05	-1.33 ± 0.04

simulations in acetonitrile as the solvent: $\Delta G_1 - \Delta G_2$ is -1.55 kcal/mol and -1.33 kcal/mol in the absence and in the presence of counterions, respectively.

Discussion

We attempted to simplify the supramolecular system in order to study it by theoretical methods. Emphasis was therefore placed on elucidating the behavior of the pseudorotaxanes, precursors of the [2]rotaxane **1**, which have been studied experimentally by J. F. Stoddart and co-workers.²⁶ The AMBER approach allows a sufficiently rigorous treatment of the electrostatics by adjusting the atomic partial charges with respect to molecular electrostatic potentials derived by quantum mechanical methods. The accurate representation of the electronic charge distribution in a tetracationic system like cyclobis-(paraquat *p*-phenylene) is a key issue in this particular case. At the same time, we recently developed²⁵ and applied in this study an explicit solvent model of acetonitrile that meets the requirements of the force field implemented in the AMBER program. The effect of explicit solvent molecules on systems such as pseudorotaxanes has previously been considered in some modeling studies^{21b} where the experimental energy difference

between pseudorotaxanes **2** and **3** was also correctly reproduced using Monte Carlo simulations. However, the final structure for these pseudorotaxanes is far from the proposed geometry derived from NOE experiments. In fact, it adopts a geometry that allows a 2:1 inclusion complex (like in the X-ray structure shown in ref 21b). The importance of counterions is also stressed in that article. In our case, however, the structural model was simplified (and chloride ions were used instead of hexafluorophosphate ions), but a fully consistent modeling of solute-solvent interactions was developed. Furthermore, a computational protocol was tested for the modeling of pseudorotaxanes that can be further utilized for studying [2]rotaxanes.

The FEP treatment of the pseudorotaxanes **2** and **3** yielded, in a manner more accurate than other approaches can provide, estimates for the free energy changes during the complexation processes of the benzidine and the 4,4'-biphenol substrates with the tetracationic cyclophane using acetonitrile as a solvent in the simulations. This study was preceded by simulations in the gas phase and in a water solution, which served as benchmark tests for comparing the quality of the modeling study in acetonitrile. Qualitative agreement of the results in the gas phase with the experimental data exists only when chloride ions are included in the simulation. This indicates the importance of taking into consideration an electrostatic counteraction to the tetracationic portion of the cyclophane.

The results from the FEP simulations in water and in the presence of Cl^- counterions differ from those experimentally observed in acetonitrile solution.²⁶ The free energy difference associated with the mutation of the benzidine residue into 4,4'-biphenol in water may be higher than the free energy difference of the process of mutation of pseudorotaxane **2** into **3**. The closure of the thermodynamic cycle with the reactions of complexation

of each residue with the cyclophane macrocycle allows us to relate the data obtained computationally to the stability of each inclusion complex. In this way, on the basis of the theoretical data, we can conclude that the association constant for the complex with benzidine (**2**) is smaller than that for the complex with the 4,4'-biphenol substrate, when the experiment is carried out in aqueous solution. The validity of this conclusion is supported by the fact that using the same force field, and following the same simulation protocol, we arrived at a correct estimate of the parameters of the complexation process in acetonitrile solution. For a weak point acting against such an interpretation has to be looked for within the boundary conditions imposed on the computational experiments in the gas phase and in water, namely, the utilization of distance restrictions in order to prevent dissociation during the simulations. We assume that these distance restrictions do not noticeably affect the values of the free energy changes, because the system retains sufficient flexibility during the FEP simulations (the restrictions are on a limited number of degrees of freedom).

When the solvent model developed for acetonitrile was used in the simulations, then, irrespective of the choice of method for estimating the partial charges (HF/6-31G* vs HF/6-311+G*) or of the presence or absence of counterions, the experimental association constants were qualitatively and quantitatively reproduced. Thus, the FEP simulations, with chloride ions included and charges for acetonitrile derived from HF/6-31G* computations, gave the qualitatively correct result for the more stable complex with benzidine, although with the tendency of enhancing the energy of complexation (-1.95 kcal/mol).³⁵ When charges from HF/6-311+G* computations were implemented in the model, then the experimental estimate was more accurately reproduced: -1.33 kcal/mol vs -1.2 kcal/mol (experimental).

Another aspect that deserves comment is the reproduction of the experimental geometries proposed for complexes **2** and **3** in acetonitrile solution.²⁶ Longer

simulation times can provide more accurate average geometries: the system will have more opportunities to traverse larger parts of the configurational space of the complex. We will then be able to identify more accurately the distribution of the aromatic rings of the two substrates relative to the center of the cyclophane cavity. The two pseudorotaxanes portrayed different tendencies: the benzidine alternates the occupancy of the center of the cavity with the two aromatic rings with a higher frequency than the 4,4'-biphenol.

Conclusions

The computed data for the isolated molecules and for pseudorotaxanes **2** and **3** indicate that the computational model developed in this work can reproduce experimental results. The next step has to be the application of this approach to more complex systems such as [2]rotaxane **1**, in which case the benzidine and the 4,4'-biphenol units are inserted within the dumbbell, and the macrocyclic bead moves back and forth between them.

We conclude, therefore, that the AMBER force field with RESP charges and the explicit solvent model for acetonitrile²⁵ provide a useful computational scheme for studying the pseudorotaxanes of benzidine (**2**) and 4,4'-biphenol (**3**) and that these can further be applied for modeling the [2]rotaxane **1**.

Acknowledgment. The authors are grateful to CESCA-C⁴ for allocating computational time. Financial support has been obtained from the Ministerio de Ciencia y Tecnología (Spain), through Grant PPQ2000-0369. We thank CIRIT (Generalitat de Catalunya) for a Visiting Professor grant to P.I., and the UAB for a fellowship awarded to X.G.

Supporting Information Available: Full set of parameters used in the molecular dynamics simulations with AMBER provided in one table. This material is available free of charge via the Internet at <http://pubs.acs.org>.

JO0265636